Real-Time IMEP Estimation and Control Using an In-Cylinder Pressure Sensor for a Common-Rail Direct Injection Diesel Engine

Seungsuk Oh
e-mail: seungsukoh@gmail.com

Junsoo Kim
e-mail: junskys@gmail.com

Byounggul Oh
e-mail: obgg@hanyang.ac.kr

Kangyoon Lee
e-mail: bbikeman@gmail.com

Myoungho Sunwoo[1]
Professor
e-mail: msunwoo@hanyang.ac.kr

Department of Automotive Engineering,
Hanyang University,
17 Haengdang-dong, Seongdong-gu,
Seoul 133-791, Republic of Korea

An in-cylinder pressure-based control method is capable of improving engine performance, as well as reducing harmful emissions. However, this method is difficult to be implemented in a conventional engine management system due to the excessive data acquisition and long computation time. In this study, we propose a real-time indicated mean effective pressure (IMEP) estimation method using cylinder pressure in a common-rail direct injection diesel engine. In this method, difference pressure integral (DPI) was applied to the estimation. The DPI requires only 180 pressure data points during one engine cycle from top dead center to bottom dead center when pressure data are captured at every crank angle. Therefore, the IMEP can be estimated in real time. To further reduce the computational load, the IMEP was also estimated using DPI at 2 deg, 3 deg, and 4 deg crank angle resolutions. Furthermore, based on the estimated IMEP, we controlled IMEP using a radial basis function network and linear feedback controller. As a result of the study, successful estimation and control were demonstrated through engine experiments. [DOI: 10.1115/1.4002250]

Keywords: cylinder pressure, indicated mean effective pressure (IMEP) estimation, difference pressure integral (DPI), torque control

1 Introduction

Stringent emission regulations and increasing requirements for fuel economy and engine performance have led to the growing complexity of engine control systems and integration with transmission and vehicle dynamics control systems [1,2]. In order to control more complex and integrated engine systems effectively, an indicator that represents engine performance is required. Engine torque is a promising candidate for such a performance indicator because it is directly related to the combustion process and engine performance [3]. For this reason, torque-based engine control has been widely researched [1–7].

To achieve precise torque-based engine control, obtaining accurate engine torque data is important. There have been several methods of indicated torque estimation based on estimation method or sensor type.

Kim et al. [8], Rizzoni [9], Citron et al. [10], Ginoux et al. [11], and Taraza [12] proposed a torque estimation method using instantaneous crank angle fluctuation. This method employs a dynamic model of the shafting and frequency spectrum of the measured speed. Although this estimation method is simple and easy to implement, it is inaccurate [11,13].

Sobel et al. [14] suggested a torque measurement method based on a torque meter. The torque meter measures the torsion, proportional to engine torque, between the flywheel and the crankshaft. Therefore, this method can directly measure engine torque. However, applying the torque meter to a commercial vehicle is difficult due to high cost and poor reliability [5,11,15].

Engine torque can also be computed from indicated mean effective pressure (IMEP) using an in-cylinder pressure sensor [16]. Using this approach, although it is possible to obtain more accurate torque than the methods above, it cannot be implemented in a conventional engine management system due to the high cost of an in-cylinder pressure sensor and the excessive computational load of cylinder pressure data processing and IMEP calculations [17]. However, the high cost problem has been solved by a sensor company; as a consequence, a passenger car equipped with the in-cylinder pressure sensors has been mass produced in 2008 [18]. Therefore, only excessive computational load remains a problem. In order to calculate IMEP from the cylinder pressure data, 720 cylinder pressure data acquisitions for each cylinder are required if cylinder pressure is captured at each crank angle (CA). In addition, IMEP calculation requires a computational load of 720 additions and 721 multiplications. Such excessive data acquisitions and computations are currently difficult to be implemented into a conventional engine management system. Thus, an IMEP obtaining method that can be performed in real-time is indispensable.

This paper presents a real-time IMEP estimation algorithm for torque-based engine control using in-cylinder pressure. In the IMEP estimation algorithm, a difference pressure integral (DPI) [19] was applied to the estimation. The DPI is computed from the simple addition of the difference pressure between the firing pressure and motoring pressure at every CA from top dead center (TDC) to bottom dead center (BDC) [19,20]. This DPI requires only 180 pressure data points during one engine cycle. Therefore, the amount of data acquisition is remarkably reduced. Using the DPI, we propose a simple linear IMEP estimation equation to achieve less computational load. Consequently, the proposed estimation algorithm can be implemented in a conventional engine management system.

[1]Corresponding author.

Contributed by the IC Engine Division of ASME for publication in the JOURNAL OF ENGINEERING FOR GAS TURBINES AND POWER. Manuscript received December 15, 2009; final manuscript received July 16, 2010; published online February 14, 2011. Assoc. Editor: Christopher J. Rutland.

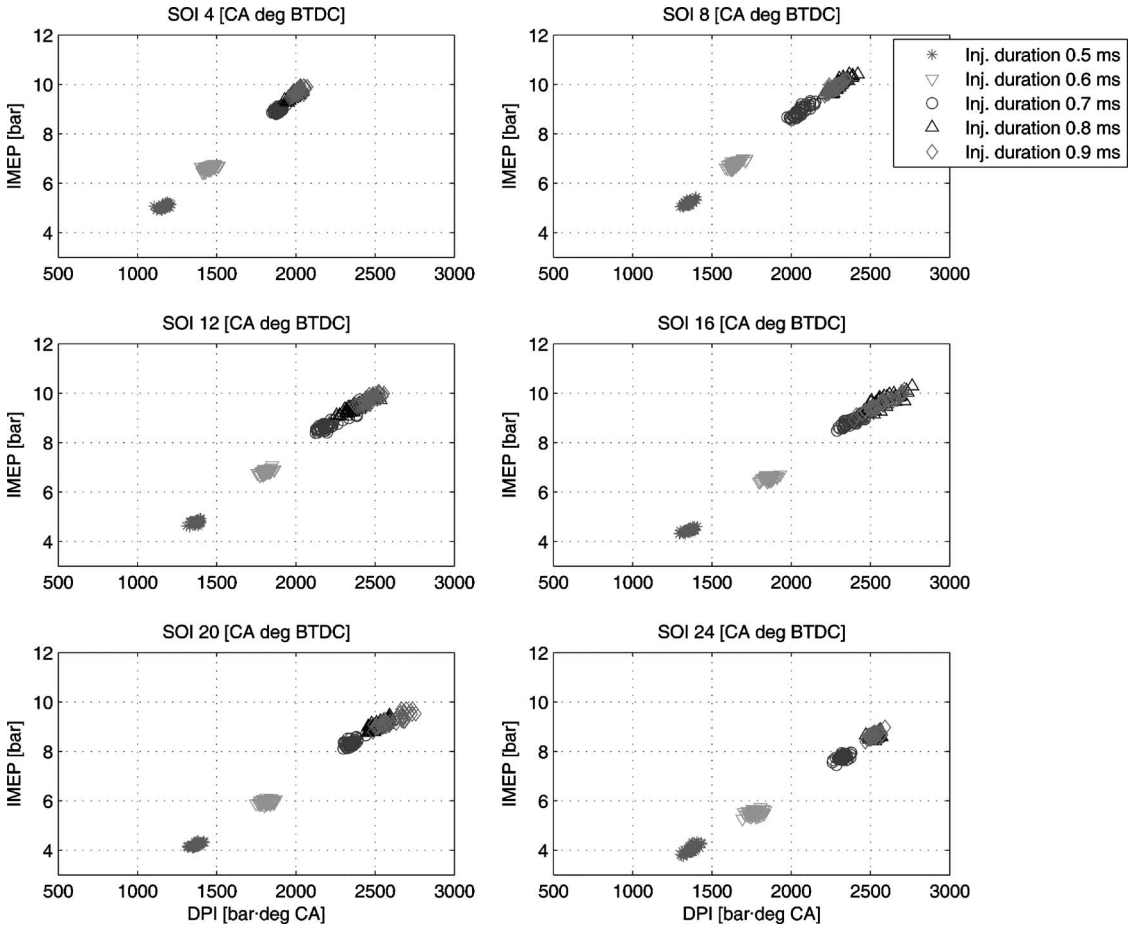

Fig. 1 IMEP with respect to DPI (2000 rpm, fuel-rail pressure of 600 bars, waste gate fully opened, without EGR)

Based on estimated results, we implemented a radial basis function network feedforward controller and PI feedback controller to check the feasibility of IMEP control. As a sequence, IMEP estimation results showed good performance as an indicator so that IMEP was closely followed the desired IMEP.

This paper consists of three sections. The IMEP estimation algorithm using DPI and the offline and online estimation results are described in Sec. 2. From the estimation results, Sec. 3 proposes an IMEP controller structure and shows the validation from experimental results. Finally, conclusions are discussed in Sec. 4.

2 IMEP Estimation

2.1 Estimation Method With Difference Pressure Integral. The DPI was selected as the pressure variable for IMEP estimation since DPI has a one-to-one correspondence with IMEP, as shown in Fig. 1. DPI was introduced by Herden and Matthias in 1994 [19,20] and is defined as

$$\mathrm{DPI} = \sum_{k=0\ \mathrm{degATDC}}^{180\ \mathrm{degATDC}} DP(k) \tag{1}$$

where DP indicates the difference pressure between firing cylinder pressure and motoring cylinder pressure. In this study, premeasured motoring pressure was used at 1500 rpm, 2000 rpm, and 2500 rpm. In order to compensate the motoring pressure during different engine operating conditions or transient engine operations, we obtained a motoring pressure using Eq. (2).

$$P_{\mathrm{motoring}} = \frac{P_{\mathrm{firing}}(90\ \mathrm{deg\ CA\ BTDC})}{P_{\mathrm{premeasured\ motoring}}(90\ \mathrm{deg\ CA\ BTDC})} \times P_{\mathrm{premeasured\ motoring}} \tag{2}$$

where P_{motoring}, P_{firing}, and $P_{\mathrm{premeasured\ motoring}}$ indicate motoring pressure, firing cylinder pressure, and premeasured motoring pressure, respectively.

In order to analyze the relationships between IMEP and DPI, cylinder pressure data were gathered, and both IMEP and DPI were calculated during 50 consecutive cycles under different steady state operating conditions: fuel-rail pressure of 600 bars, waste gate fully opened, without EGR, engine speeds from 1500 rpm to 2500 rpm, injection timings from 4 BTDC CA to 24 BTDC CA, and injection durations from 0.5 ms to 0.9 ms. Figure 1 depicts the calculation results of IMEP and DPI at 2000 rpm. As illustrated in Fig. 1, DPI and IMEP increased as injection duration increased and DPI showed a linear relationship with IMEP at each injection timing condition. The linear relationship can be expressed as

$$\mathrm{IMEP} = f_a(\mathrm{SOI},\mathrm{rpm}) \times \mathrm{DPI} + f_b(\mathrm{SOI},\mathrm{rpm}) \tag{3}$$

In Eq. (3), the gradient f_a and vertical-intercept f_b are determined by lookup tables, as shown in Fig. 2. The lookup tables were created through experiments under different start of injections (SOIs) and engine speed conditions.

Compared with conventional IMEP calculation, the estimation equation has a small amount of computation. As outlined in Table 1, the conventional IMEP calculation method requires 2880 cyl-

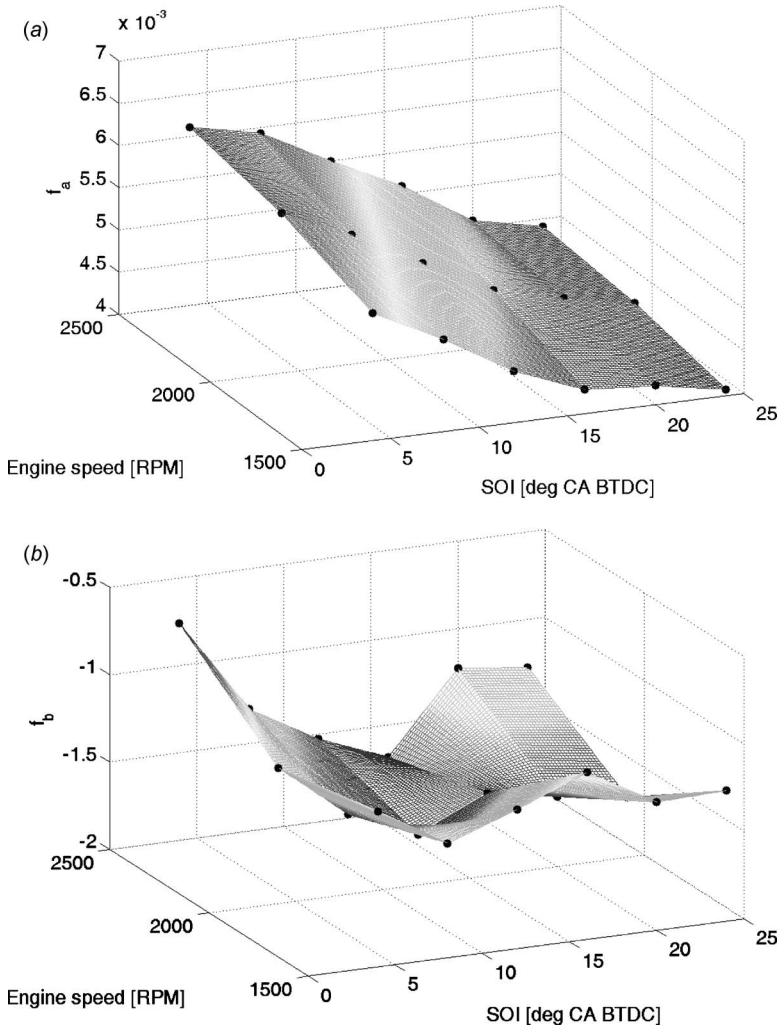

Fig. 2 Lookup tables for the coefficient of estimation equation

inder pressure data points if pressure data are captured at every crank angle and that IMEP calculation method includes 2880 additions and 2884 multiplications for four cylinders. In contrast, the proposed algorithm herein requires only 720 cylinder pressure data points per cylinder for estimation, with only 1464 additions and one multiplication. This remarkable reduction makes it possible to obtain IMEP in real-time.

2.2 Influences of the Calculation Range of DPI. SOI, TDC, exhaust valve open (EVO), and BDC are special points that largely affect difference pressure changes. To analyze the effect of DPI calculation range according to the events on IMEP estimation, we obtained a root mean squared error (RMSE) as calculation ranges change: SOI to EVO, SOI to BDC, TDC to EVO, and TDC to BDC. The RMSE represented the difference between values obtained via the estimator versus calculated from the cylinder pressure data. RMSE is given as

$$\mathrm{RMSE} = \sqrt{\frac{\sum_{k=1}^{n} [(\mathrm{IMEP}_{\mathrm{estimated}} - \mathrm{IMEP}_{\mathrm{calculated}})^2]}{n}} \tag{4}$$

where $\mathrm{IMEP}_{\mathrm{estimated}}$ and $\mathrm{IMEP}_{\mathrm{calculated}}$ represent the IMEP estimated using Eq. (3) and the IMEP calculated using Eq. (5), respectively.

Table 1 Data acquisition, computational load, and computation time (four-cylinder engine)

	IMEP	IMEP_2	IMEP_4	IMEP_8	IMEP_{12}	IMEP_{16}	DPI	DPI_2	DPI_3	DPI_4
No. of pressure data captures (per cycle)	2880	1440	720	360	240	180	720	360	240	180
No. of additions (per cycle)	2880	1440	720	360	240	180	1464	744	504	384
No. of multiplications (per cycle)	2884	1444	724	364	244	184	4	4	4	4
RMSE (bar)	-	0.0432	0.0806	0.1407	0.2021	0.3098	0.1088	0.1307	0.1322	0.1578
Computation time 16 MHz (ms)	14.436	7.200	3.608	1.804	1.204	0.904	2.356	1.180	0.792	0.600
Computation time 32 MHz (ms)	7.208	3.608	1.808	0.901	0.601	0.452	1.176	0.591	0.396	0.299
Computation time 64 MHz (ms)	3.600	1.804	0.904	0.449	0.300	0.225	0.588	0.295	0.198	0.149
Computation time 128 MHz (ms)	1.804	0.900	0.448	0.224	0.150	0.112	0.294	0.147	0.099	0.074

Table 2 Influence of DPI calculation range on RMSE

	SOI to EVO	SOI to BDC	TDC to EVO	TDC to BDC
RMSE	0.1749	0.1648	0.1159	0.1088

$$\text{IMEP}_{\text{calculated}} = \frac{\Delta\theta}{V_s}\sum_{k=1}^{720} p(k)\frac{dV(k)}{d\theta} \tag{5}$$

where $\Delta\theta$, $p(k)$, $V(k)$, and V_s indicate crank angle resolution in-cylinder pressure at crank angle position k cylinder volume at crank angle position k and cylinder swept volume, respectively.

Table 2 shows the results of RMSE. Despite different SOIs being considered, the IMEP estimations with DPIs calculated from SOI showed large RMSE over 0.16. On the other hand, DPI during expansion stroke (TDC to BDC) well-estimated IMEP with the lowest RMSE of 0.1088 and the DPI from TDC to EVO also showed a small RMSE of 0.1159. Although estimated IMEP using DPI from TDC to EVO showed a little larger RMSE than the RMSE of DPI during expansion stroke, it has the advantage of reductions of data acquisitions and computational load.

2.3 Influences of Measurement Error on IMEP Estimation. A piezoelectric pressure transducer is sensitive to thermal shock. Thermal shock of the pressure transducer causes pressure offset in in-cylinder pressure measurements [21–26]. In this section, we analyzed the influence of the pressure offset on IMEP estimation error. Cylinder offset affects the error in estimation of motoring pressure. Consequently, the offset results in DPI calculation error causes IMEP estimation errors. In this analysis, therefore, to measure cylinder pressure accurately, we applied a modified least-squares pegging method, proposed by Lee et al. [24,26]. Based on the pegged cylinder pressure, we added cylinder pressure offset from 0.1 to 0.5 and calculated RMSE of all experimental conditions.

Table 3 The influence of cylinder pressure offset on RMSE

Pressure offset (bar)	0	0.1	0.2	0.3	0.4	0.5
RMSE	0.1088	0.1292	0.1567	0.1909	0.2292	0.2696

Table 4 Specifications of the experimental system

Description		Specification
Engine	Engine type	In-line single overhead camshaft (SOHC) turbocharged CRDI
	Number of cylinders	4
	Displacement volume	1991 cc
	Compression ratio	17.3
Cylinder pressure sensor		Glow plug type piezoelectric pressure transducer (Kistler)
Engine controller		MicroAutoBOX (dSPACE)

Table 3 shows the RMSE when the pressure offset varies from 0.1 bar to 0.5 bar. As the pressure offset increases from 0.1 bar to 0.5 bar, the RMSE was also increased from 0.1292 to 0.2696. The estimation results are sensitive to cylinder pressure offset and, accordingly, cylinder pressure pegging or accurate motoring pressure estimation is required.

2.4 Computation Time Measurement. In order to check the validity of the proposed IMEP estimation algorithm in real-time, the computation times of the proposed IMEP estimation algorithm and the conventional IMEP calculation method were measured with a MPC5554 PowerPC microcontroller, designed for engine management systems, at its best calculation condition using the signal processing extension auxiliary processing unit (SPE-APU). The SPE-APU provides a set of single instruction multiple data (SIMD) instructions that involves performing the same operation on multiple data elements stored in a single 64 bit register. Through the implementation of SIMD instructions, the SPE-APU enables fast floating point operation. As listed in Table 1, 7.208 ms were needed to calculate the IMEP for four cylinders during 1 cycle when the system clock of the microcontroller was 32 MHz. In comparison, the proposed algorithm estimated the IMEP takes 1.176 ms, which is about 1/6 of the duration of the conventional IMEP calculation method. This reduction in computation time of control applications is important because many applications, such as fuel system control and air system control, have to be embedded to one engine control unit (ECU).

2.5 Experimental Setup. A 2 l, four-cylinder common-rail direct injection (CRDI) engine was used for the experiments. The engine was connected to an eddy current engine dynamometer and a glow plug type piezoelectric pressure transducer was added to one engine cylinder. To measure cylinder pressure at a certain crank angle degree, TDC position was determined by using an incremental rotary encoder that generates 3600 pulses per revolution and 1 pulse per revolution.

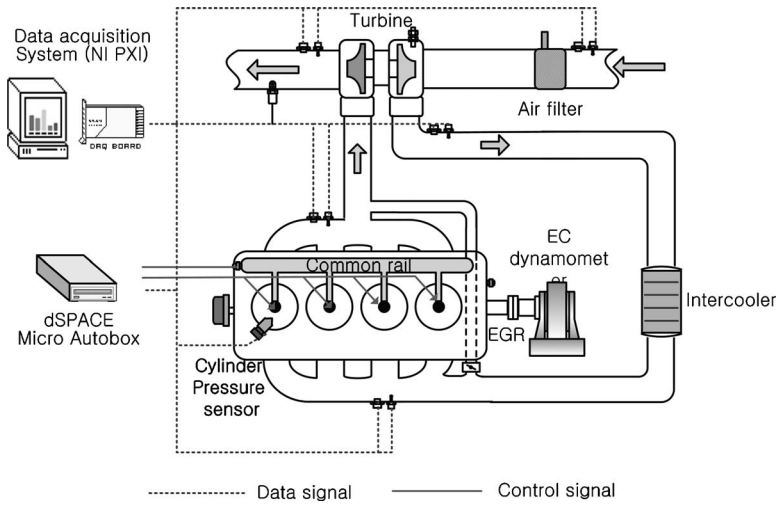

Fig. 3 Experimental setup

A National Instrument PXI system was employed for data acquisition and a dSPACE MicroAutoBox was used to adjust experimental conditions. Detailed specifications for the experimental system are described in Table 4 and in Fig. 3.

2.6 Experimental Results of the IMEP Estimation. Engine experiments were carried out to validate the proposed IMEP estimation method. Cylinder pressure data were measured during ten consecutive cycles under the following engine conditions: fuel-rail pressure of 600 bars, waste gate fully opened, without EGR, engine speeds of 1500 rpm, 1750 rpm and 2500 rpm, injection timings of 4–24 deg CA BTDC, and injection durations of 0.5–0.9 ms. Based on the captured cylinder pressure data, IMEP was estimated offline using Eq. (3), as depicted in Fig. 4. Consequently, the estimation results showed a good estimation results with a small RMSE of 0.1088.

An IMEP estimator should be robust enough to withstand changes in operating conditions and external disturbances. In order to verify the robustness of the estimation method, online estimation was also performed when injection duration changed from 0.5 ms to 0.8 ms for 20 engine cycles at 1500 rpm and 2000 rpm. As shown in Fig. 5, the IMEP was successfully estimated with errors less than 0.2 bar for all except one engine cycle during each transient condition.

2.7 Experimental Results of the IMEP Estimation Using DPI at Intervals. IMEP is insensitive to the in-cylinder pressure sampling rate [27,28]. Even if the IMEP is calculated with more than 1 deg CA interval, it remains reliable without serious errors and helps reduce the computational load. Table 1 shows the RMSE of the IMEP calculations when pressure data were sampled at every 1 deg, 2 deg, 3 deg, and 4 deg CA, which were defined as IMEP, $IMEP_2$, $IMEP_3$, and $IMEP_4$ respectively. As shown in Table 1, even though the sampling resolution was 4 deg CA, RMSE was 0.0806 bar. Compared with $IMEP_4$, the estimation results using DPI, which requires the identical number of pressure data sampling, have almost the same RMSE. In addition, the computation time of the IMEP estimation using DPI is 2/3 the computation time of $IMEP_4$.

IMEP was also estimated with DPI sampled in the same manner as with the sampling of $IMEP_2$, $IMEP_3$, and $IMEP_4$. DPI_2, DPI_3, and DPI_4 were defined as IMEP estimations when the sampling resolutions were 2 deg, 3 deg, and 4 deg, respectively. As a result of these estimations, based on the same number of data captures, the computation times of DPI, DPI_2, DPI_3, and DPI_4 are 2/3 the computation times of $IMEP_4$, $IMEP_8$, and $IMEP_{12}$ respectively, as shown in Figs. 6 and 7. In addition, DPI_2, DPI_3, and DPI_4 showed smaller RMSE errors than $IMEP_8$, $IMEP_{12}$, and $IMEP_{16}$, as illustrated in Fig. 8.

3 IMEP Control

3.1 Structure of IMEP Controller. In order to evaluate DPI as a control variable, we designed an IMEP controller. The IMEP controller consisted of a feedforward controller to improve the set-point response and a feedback controller for reduction of the effect of disturbances, as shown in Fig. 9.

A feedforward controller was implemented to perform input-output mapping using a radial basis function network (RBFN). The RBFN was introduced by Moody and Darken in 1989 and is a valuable tool for nonlinear mapping [29]. The RBFN consists of three layers: an input layer, a hidden layer, and an output layer. The first layer, the input layer, is composed of an input vector $x = [\mathrm{SOI}, \mathrm{rpm}, \mathrm{DPI}]$, where DPI is obtained by the inverse of Eq. (3). The second layer, the hidden layer, performs nonlinear transformation from the input vector to hidden space and is activated by a Gaussian transfer function, according to the following equation:

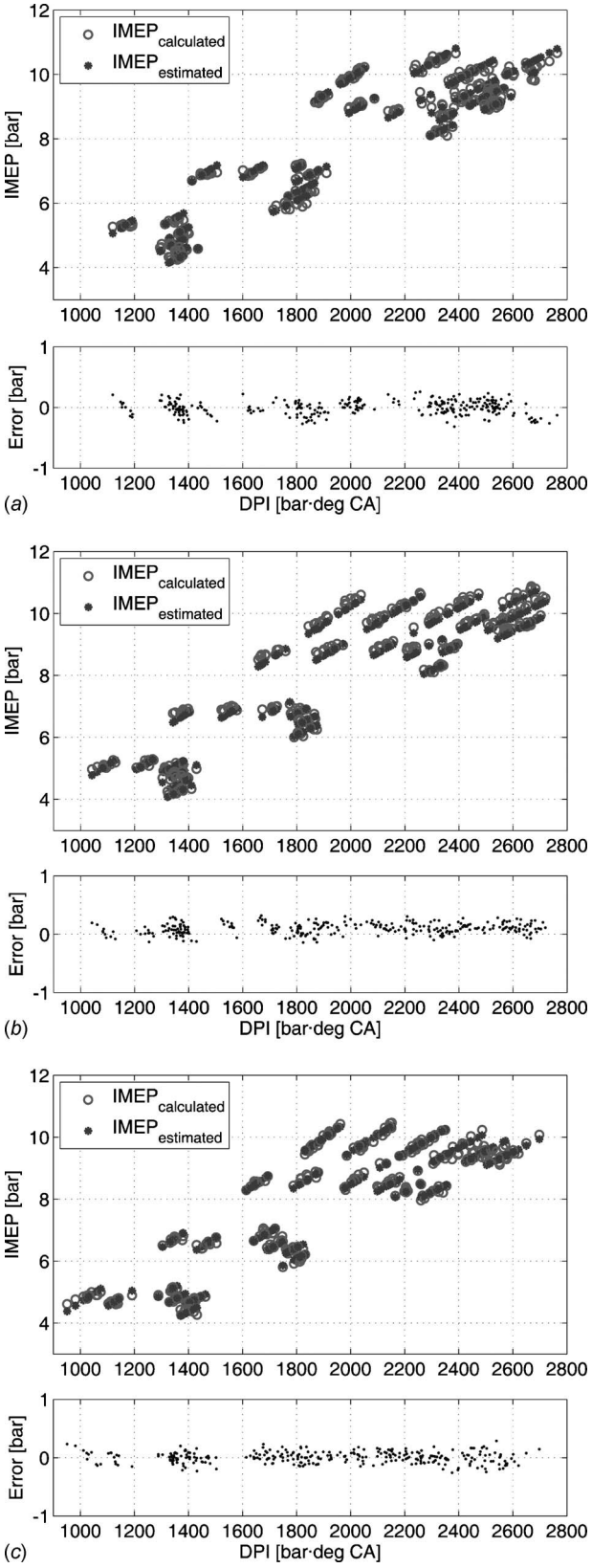

Fig. 4 Offline IMEP estimation experimental results (fuel-rail pressure of 600 bars, waste gate fully opened, without EGR)

$$h_j(x) = \exp\left(-\frac{\|x - m_j\|^2}{\sigma^2}\right) \tag{6}$$

where x, m_j, and σ represent the input vectors to the network, and the mean and variance of jth Gaussian function, respectively.

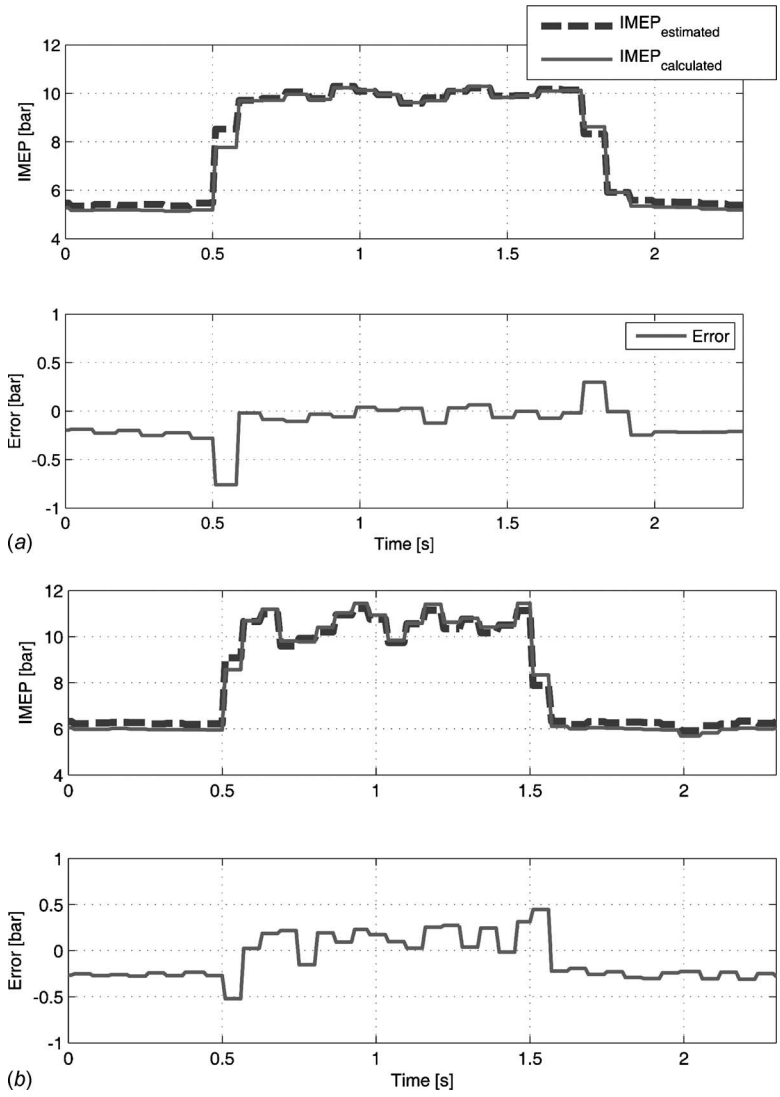

Fig. 5 Online IMEP estimation experimental results

From this hidden layer, output can be obtained by the linearly weighted sum of h_j as written in

$$y(x) = \sum_{j=1}^{m} w_j h_j(x) \tag{7}$$

where y is the injection duration and w_j is the jth weight obtained by training with the three inputs of SOI, engine speed, and DPI, and the one output of injection duration.

Finally, combined with the feedback PI controller, the injection duration at the kth instant can be derived as

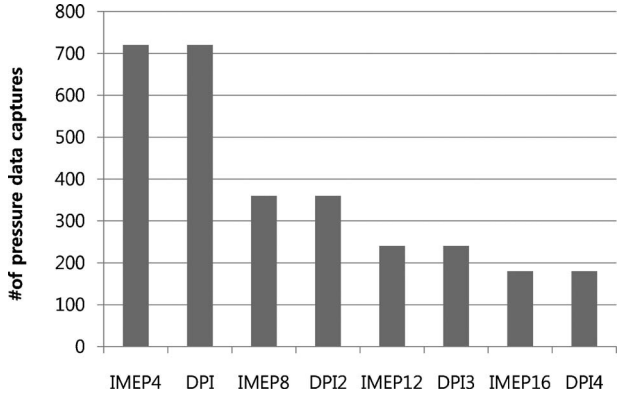

Fig. 6 The number of pressure data captures

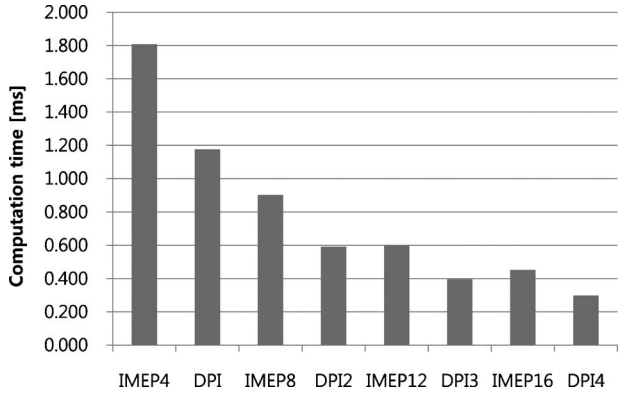

Fig. 7 Computation time

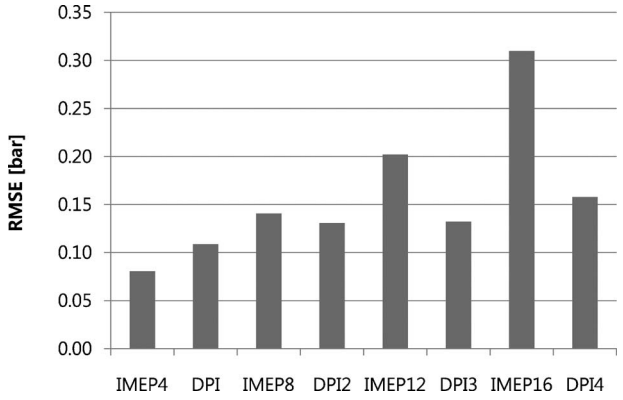

Fig. 8 RMSE

$$\mathrm{Inj}(k) = \mathrm{Inj}_{FF}(k) + \mathrm{Inj}_{FB} = \mathrm{Inj}_{FF}(k) + K_p e(k) + K_i \sum_{k=0}^{k-1} e(k) \quad (8)$$

where Inj, Inj_{FF}, Inj_{FB}, K_p, and K_i are the injection duration output, the injection duration output from feedforward controller, the injection duration output from feedback controller, and the proportional and integral gain of the PI controller, respectively. In addition, $e(k)$ indicated the error between desired IMEP and estimated IMEP. The estimated IMEP is calculated from an IMEP estimator using DPI and Eq. (3).

3.2 Experimental Results of IMEP Control. Figure 10 depicts the engine experimental results of the IMEP estimation and control under 1500 rpm and 2000 rpm with a SOI of 12 deg CA. At each engine speed, as the desired IMEP changed from 3 bars to 6 bars during 80 engine cycles and then changed again from 6 bars to 3 bars, the IMEP successfully followed the desired IMEP with a fast settling time of 200 ms.

4 Conclusions

A cylinder pressure-based control method is capable of direct combustion feedback control. However, this method requires a large amount of pressure data acquisition and computation. As such, the method is difficult to embed into a real-time controller. In this study, a novel real-time IMEP estimation method, which can be applied to control applications, such as torque-based control and cylinder-by-cylinder variation control, is proposed. The IMEP estimation method required only 180 pressure data points per one cylinder. Nevertheless, the estimation method showed sufficient accuracy with a RMSE of 0.1088 bar. Results are summarized as follows.

(1) Under various operating conditions, the IMEP was precisely estimated with a RMSE of only 0.1088 bar.
(2) The proposed algorithm has a short computation time, which is 1/6 of the conventional IMEP calculation method. This faster computation time enables real-time IMEP estimation and allows the method to be embedded into a conventional real-time controller.
(3) IMEP was estimated with different sampling resolutions: 2 deg, 3 deg, and 4 deg CA. Despite the small amount of sampling data, IMEP was successfully estimated. As the number of samples is decreased, the computational load decreased enough so that the method can be easily implemented in conventional engine management systems.
(4) A RBFN feedforward and linear feedback controller were implemented to control the IMEP effectively, as indicated by a settling time of 200 ms.

Our future work will deal with cylinder-by-cylinder torque control and real-time IMEP estimation under various conditions, such as engine aging, various common-rail pressures, EGR rates, and boosting conditions. In addition, we are investigating motoring pressure estimation algorithms, which are robust to pressure offset errors. Furthermore, we plan to control brake mean effective pressure with the IMEP estimation results considering a friction mean effective model according to engine operating conditions.

Acknowledgment

This work (research) is financially supported by the Ministry of Knowledge Economy (MKE) and Korea Institute for Advancement in Technology (KIAT) through the Workforce Development Program in Strategic Technology and was partially supported by the Brain Korea 21 Project in 2010.

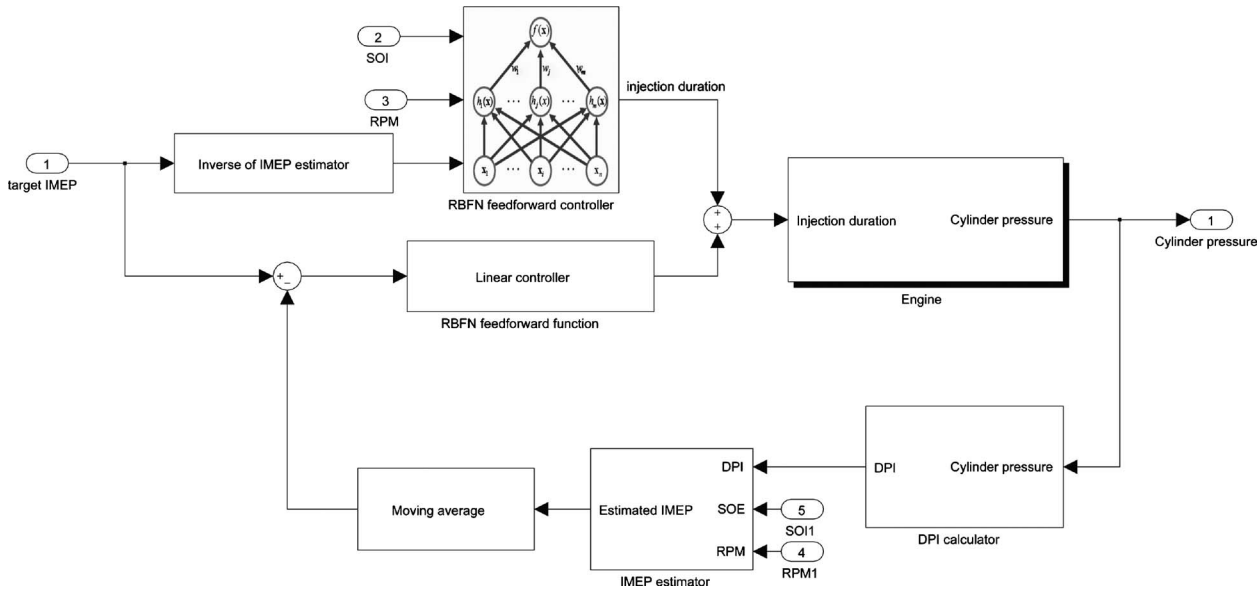

Fig. 9 Schematic of IMEP estimation and control system

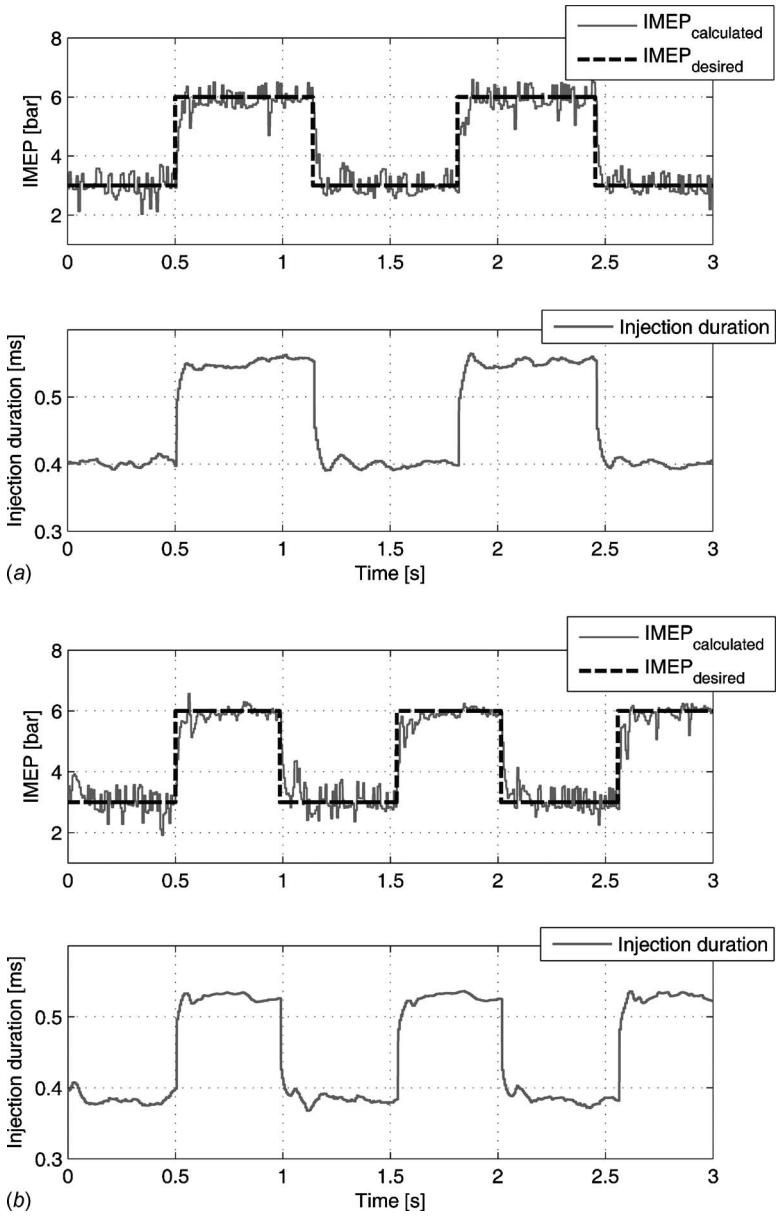

Fig. 10 IMEP control results

Nomenclature

h_j = the jth basis function
Inj_{FB} = injection duration output from feedback controller
Inj_{FF} = injection duration output from feedforward controller
$\text{IMEP}_{\text{calculated}}$ = calculated IMEP
$\text{IMEP}_{\text{estimated}}$ = estimated IMEP
K_i = integral gain of PI controller
K_p = proportional gain of PI controller
m_j = mean of the jth Gaussian function
P_{firing} = firing pressure
P_{motoring} = motoring pressure
$P_{\text{premeasured motoring}}$ = premeasured motoring pressure
p = in-cylinder pressure
w_j = the ith weight
x = input vector of RBFN
V = volume
V_s = swept volume
θ = crank angle
σ_j = variance of the jth Gaussian function

References

[1] Livshiz, M., Kao, M., and Will, A., 2008, "Engine Torque Control Variation Analysis," SAE Paper No. 2008-01-1016.
[2] Satou, S., Nakagawa, S., Kakuya, H., Minowa, T., Nemoto, M., and Konno, H., 2008, "An Accurate Torque-Based Engine Control by Learning Correlation Between Torque and Throttle Position," SAE Paper No. 2008-01-1015.
[3] Rizzoni, G., Guezennec, Y., and Soliman, A., 2003, "Engine Control Using Torque Estimation," U.S. Patent No. 0,167,118.
[4] Heintz, N., Mews, M., Stier, G., Beaumont, A., and Noble, A., 2001, "An Approach to Torque-Based Engine Management Systems," SAE Paper No. 2001-01-0269.
[5] Jaine, T., Charlet, A., and Higelin, P., 2002, "High Frequency IMEP Estimation and Filtering for Torque Based SI Engine Control," SAE Paper No. 2002-01-1276.
[6] Livshiz, M., Kao, M., and Will, A., 2004, "Validation and Calibration Process of Powertrain Model for Engine Torque Control Development," SAE Paper No. 2004-01-0902.
[7] Chamaillard, P. H. Y., and Charlet, A., 2004, "A Simple Method for Robust Control Design, Application on a Non-Linear, and Delayed System: Engine

Torque Control," Control Eng. Pract., **12**, pp. 417–429.
[8] Kim, Y. W., Rizzoni, G., and Wang, Y. Y., 1999, "Design of an IC Engine Torque Estimator Using Unknown Input Observer," ASME J. Dyn. Syst., Meas., Control, **121**, pp. 487–493.
[9] Rizzoni, G., 1989, "Estimate of Indicated Torque From Crankshaft Speed Fluctuations: A Model for the Dynamics of the IC Engine," IEEE Trans. Veh. Technol., **38**, pp. 168–179.
[10] Citron, S. J., O'Higgins, J. E., and Chen, L. Y., 1989, "Cylinder-By-Cylinder Engine Pressure and Pressure Torque Waveform Determination Utilizing Speed Fluctuations," SAE Paper No. 890486.
[11] Ginoux, S., and Champoussin, J.-C., 1997, "Engine Torque Determination by Crank Angle Measurements: State of the Art, Future Prospects," SAE Paper No. 970532.
[12] Taraza, D., 1993, "Possibilities to Reconstruct Indicator Diagrams by Analysis of the Angular Motion of the Crankshaft," SAE Paper No. 932414.
[13] Lida, K., Akishino, K., and Kido, K., 1990, "IMEP Estimation From Instantaneous Crankshaft Torque Variation," SAE Paper No. 900617.
[14] Sobel, J., Jeremiasson, J., and Wallin, C., 1996, "Instantaneous Crankshaft Torque Measurement in Cars," SAE Paper No. 960040.
[15] Labreuche, G., Costa, A. D., Chamaillard, Y., Charlet, A., Higelin, P., and Perrier, C., 2001, "Total Friction Effective Pressure and Torque Estimation," MECA'01.
[16] Heywood, J. B., 1988, *Internal Combustion Engine Fundamentals*, McGraw-Hill, New York.
[17] Katrašnik, T., Trenc, F., and Oprešnik, S. R., 2006, "A New Criterion to Determine the Start of Combustion in Diesel Engines," ASME J. Eng. Gas Turbines Power, **128**, pp. 928–933.
[18] Hadler, J., Rudolph, F., Dorenkamp, R., Stehr, H., Dusterdiek, T., Gilzendeger, J., Mannigel, D., Kranzusch, S., Veldten, B., Kosters, M., and Specht, A., 2008, "Volkswagen's New 2.0L TDI Engine Fulfils the Most Stringent Emission Standards," Internationales Wiener Motoren Symposium.
[19] Herden, W., and Matthias, K., 1994, "A New Combustion Pressure Sensor for Advanced Engine Management," SAE Paper No. 940379.
[20] Kleinschmidt, P., and von Garssen, H., 1994, "Process for Producing a Control Signal for the Ignition Point of an Internal Combustion Engine," German Patent No. DE 4318504.
[21] Pipitone, E., 2008, "A Comparison Between Combustion Phase Indicators for Optimal Spark Timing," ASME J. Eng. Gas Turbines Power, **130**, p. 052808.
[22] Brunt, M. F. J., and Pond, C. R., 1997, "Evaluation of Techniques for Absolute Cylinder Pressure Correction," SAE Paper No. 970036.
[23] Gilkey, J. C., and Powell, J. D., 1985, "Fuel-Air Ratio Determination From Cylinder Pressure Time Histories," ASME J. Dyn. Syst., Meas., Control, **107**, pp. 252–257.
[24] Lee, K., Kwon, M., Sunwoo, M., and Yoon, M., 2007, "An In-Cylinder Pressure Referencing Method Based on a Variable Polytropic Coefficient," SAE Paper No. 2007-01-3535.
[25] Yoon, M., Lee, K., and Sunwoo, M., 2007, "A Method for Combustion Phasing Control Using Cylinder Pressure Measurement in a CRDI Diesel Engine," Mechatronics, **17**, pp. 469–479.
[26] Lee, K., Yoon, M., and Sunwoo, M., 2008, "A Study on Pegging Methods for Noisy Cylinder Pressure Signal," Control Eng. Pract., **16**, pp. 922–929.
[27] Brunt, M. F. J., and Emtage, A. L., 1996, "Evaluation of IMEP Routines and Analysis Errors," SAE Paper No. 960609.
[28] Brunt, M. F. J., and Gordon Lucas, G., 1991, "The Effect of Crank Angle Resolution on Cylinder Pressure Analysis," SAE Paper No. 910041.
[29] Lin, C. T., and Lee, C. S. G., 1996, *Neural Fuzzy Systems*, Prentice-Hall, Englewood Cliffs, NJ.